Table S1 related to Figure 1. Demographic and clinical characteristics of the study cohort.

	CDK4/6i + AI n = 216	CDK4/6i + SERD n = 132
Age at diagnosis		
<40	54 (25.0%)	25 (18.9%)
40-49	50 (23.1%)	42 (31.8%)
50-59	67 (31.0%)	44 (33.3%)
≥60	45 (20.8%)	21 (15.9%)
Stage at diagnosis		
Stage I	34 (15.7%)	17 (12.9%)
Stage II	55 (25.5%)	47 (35.6%)
Stage III	52 (24.1%)	36 (27.3%)
Stage IV	73 (33.8%)	32 (24.2%)
Not available	2 (0.9%)	0
Histology		
Invasive ductal	149 (69.0%)	99 (75.0%)
Invasive lobular	48 (22.2%)	24 (18.2%)
Mixed ductal/lobular	13 (6.0%)	8 (6.1%)
Carcinoma NOS or other	6 (2.8%)	1 (0.8%)
Histologic grade (primary tumor)		
I-Well differentiated	4 (1.9%)	6 (4.5%)
II-Moderately differentiated	42 (19.4%)	26 (19.7%)
III-Poorly differentiated	134 (62.0%)	77 (58.3%)
Not available	36 (16.7%)	23 (17.4%)
Menopausal status at diagnosis		
Pre	97 (44.9%)	65 (49.2%)
Peri	15 (6.9%)	6 (4.5%)
Post	103 (47.7%)	60 (45.5%)
Not applicable (male%)	0	1 (0.8%)
Not available	1 (0.5%)	0
Prior lines of therapy in metastatic setting		
Median (range)	1 (0, 16)	2 (0, 11)
Sequenced sample type		
Primary	59 (27.3%)	33 (25.0%)
Metastasis	157 (72.7%)	99 (75.0%)

Abbreviations. CDK4/6i: CDK4/6 inhibitor, AI: aromatase inhibitor, SERD: selective estrogen degrader

Figure S1, related to Figure 1. Pattern, frequency, and type of genomic alterations in key breast cancer genes in 348 patients who underwent genomic profiling of the tumor using prior to start of CDK4/6i therapy.

Bars represent somatic non-synonymous mutation rate for the samples.

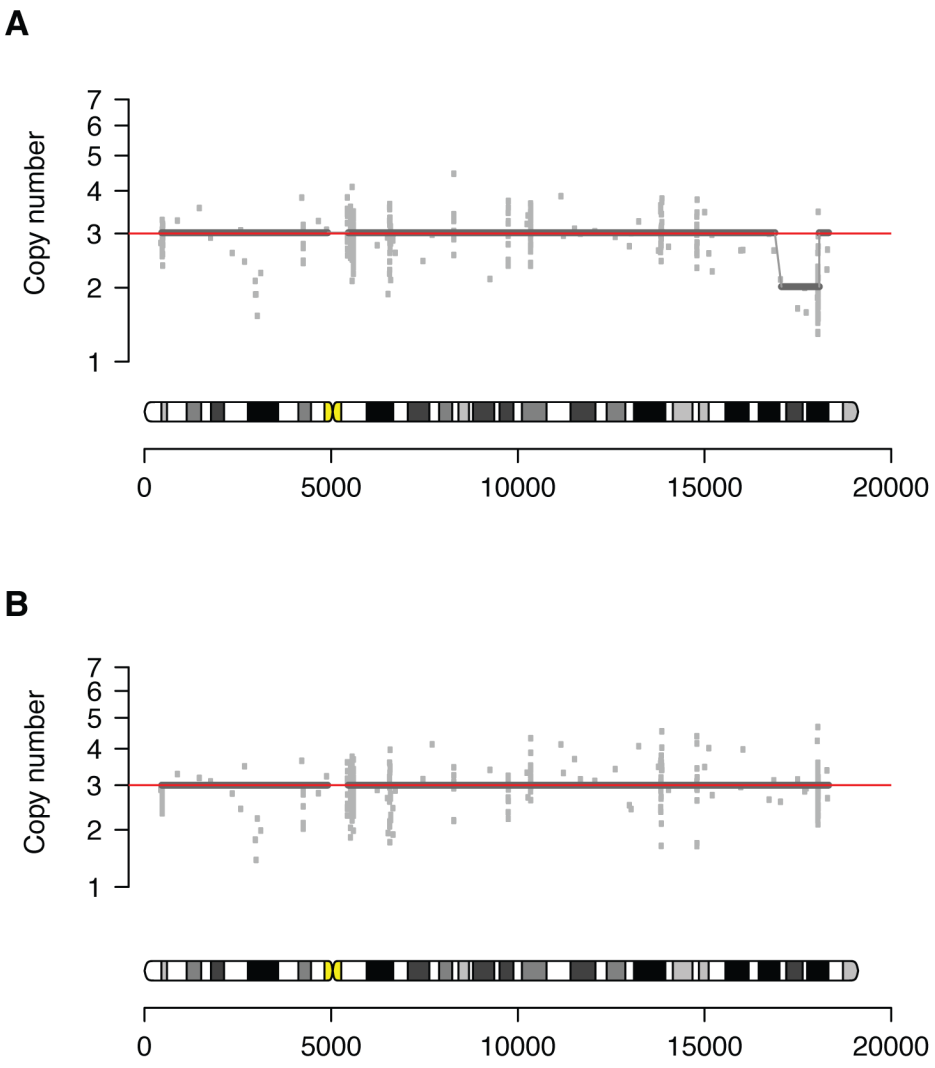

Figure S2 related to Figure 2. Estimated integer copy numbers of chromosome 4 for pre- and post-treatment tumors.

(**A**, **B**) Estimated integer copy numbers of chromosome 4 for the biopsies of the post-treatment liver metastasis of the patient with *ADAM29-FAT1* fusion (A) and the pre-treatment lung metastasis (B) presented in Figures 2D-2F. The post-treatment sample shows a copy number deletion of 4q35.2 involving *FAT1*.

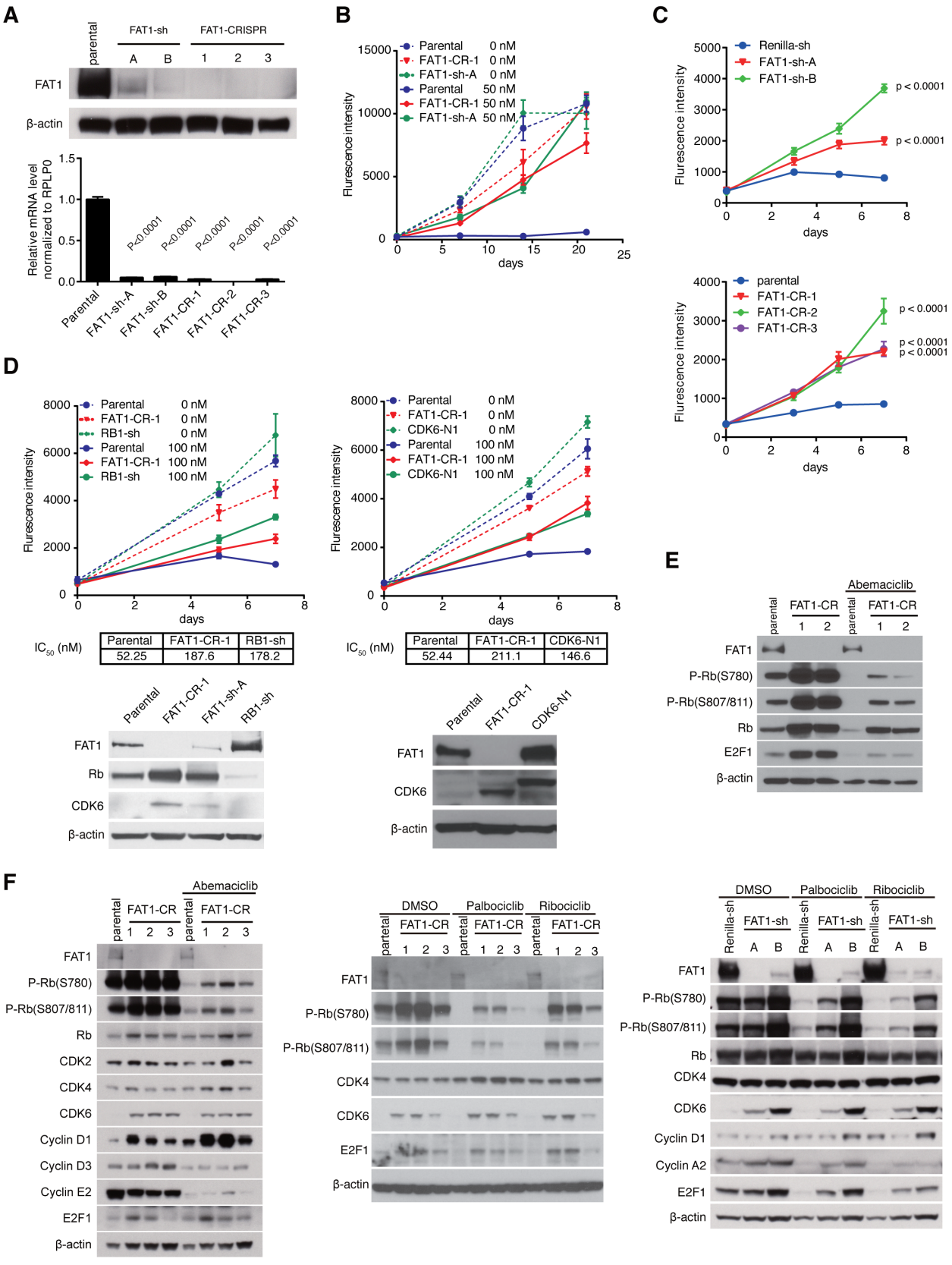
A
parental
FAT1-sh
FAT1-CRISPR
A
B
1
2
3
FAT1
β-actin
Relative mRNA level normalized to RPLP0
P<0.0001
Parental
FAT1-sh-A
FAT1-sh-B
FAT1-CR-1
FAT1-CR-2
FAT1-CR-3
B
Parental 0 nM
FAT1-CR-1 0 nM
FAT1-sh-A 0 nM
Parental 50 nM
FAT1-CR-1 50 nM
FAT1-sh-A 50 nM
Flurescence intensity
days
C
Renilla-sh
FAT1-sh-A
FAT1-sh-B
p < 0.0001
Flurescence intensity
days
parental
FAT1-CR-1
FAT1-CR-2
FAT1-CR-3
p < 0.0001
p < 0.0001
p < 0.0001
D
Parental 0 nM
FAT1-CR-1 0 nM
RB1-sh 0 nM
Parental 100 nM
FAT1-CR-1 100 nM
RB1-sh 100 nM
Flurescence intensity
days
IC50 (nM)
Parental
FAT1-CR-1
RB1-sh
52.25
187.6
178.2
Parental
FAT1-CR-1
FAT1-sh-A
RB1-sh
FAT1
Rb
CDK6
β-actin
CDK6-N1
IC50 (nM)
52.44
211.1
146.6
E
Abemaciclib
parental
FAT1-CR
1
2
FAT1
P-Rb(S780)
P-Rb(S807/811)
Rb
E2F1
β-actin
F
Abemaciclib
CDK2
CDK4
CDK6
Cyclin D1
Cyclin D3
Cyclin E2
E2F1
β-actin
DMSO
Palbociclib
Ribociclib
partetal
3
Renilla-sh
A
B
Cyclin A2

Figure S3, related to Figure 3. *FAT1* loss induces CDK6 expression and CDK4/6 inhibitor resistance in breast cancer cells.

(**A**) mRNA and protein level of FAT1 in MCF7 *FAT1* loss models. Data are represented as mean ± SD; n = 3. All p values are based on one-way ANOVA test with Dunnett's method correction, compared with parental. (**B**) Proliferation of *FAT1*-loss and parental MCF7 cells with or without 50 nM of abemaciclib treatment reveals resistance of FAT1 suppressed models. Data are represented as mean ± SD; n = 2. (**C**) Cell growth rate of FAT1-sh, FAT1-CR, Renilla-sh and parental MCF7 cells exposed to 100 nM of abemaciclib. Data are represented as mean ± SD; n = 2. All p values are based on one-way ANOVA statistical test of day 5 data with Dunnett's method correction compared with parental or Renilla-sh. (**D**) Expression of indicated proteins in parental, *FAT1*-loss, RB1 knockdown or CDK6-overexpression MCF7 cells and proliferation of these cells with or without 100 nM of abemaciclib treatment. IC_{50}s were calculated based on day 5 data of various doses of drug treatment. Data are represented as mean ± SD; n = 2. (**E**) Phospho-Rb levels and expression of indicated proteins in parental and FAT1-CR CAMA-1 cells treated with or without 100 nM of abemaciclib for 24 hours. (**F**) Phospho-Rb and expression of indicated proteins in FAT1-CR, FAT1-sh, Renilla-sh and parental MCF7 cells treated with or without 100 nM of abemaciclib, palbociclib or ribociclib for 24 hours.

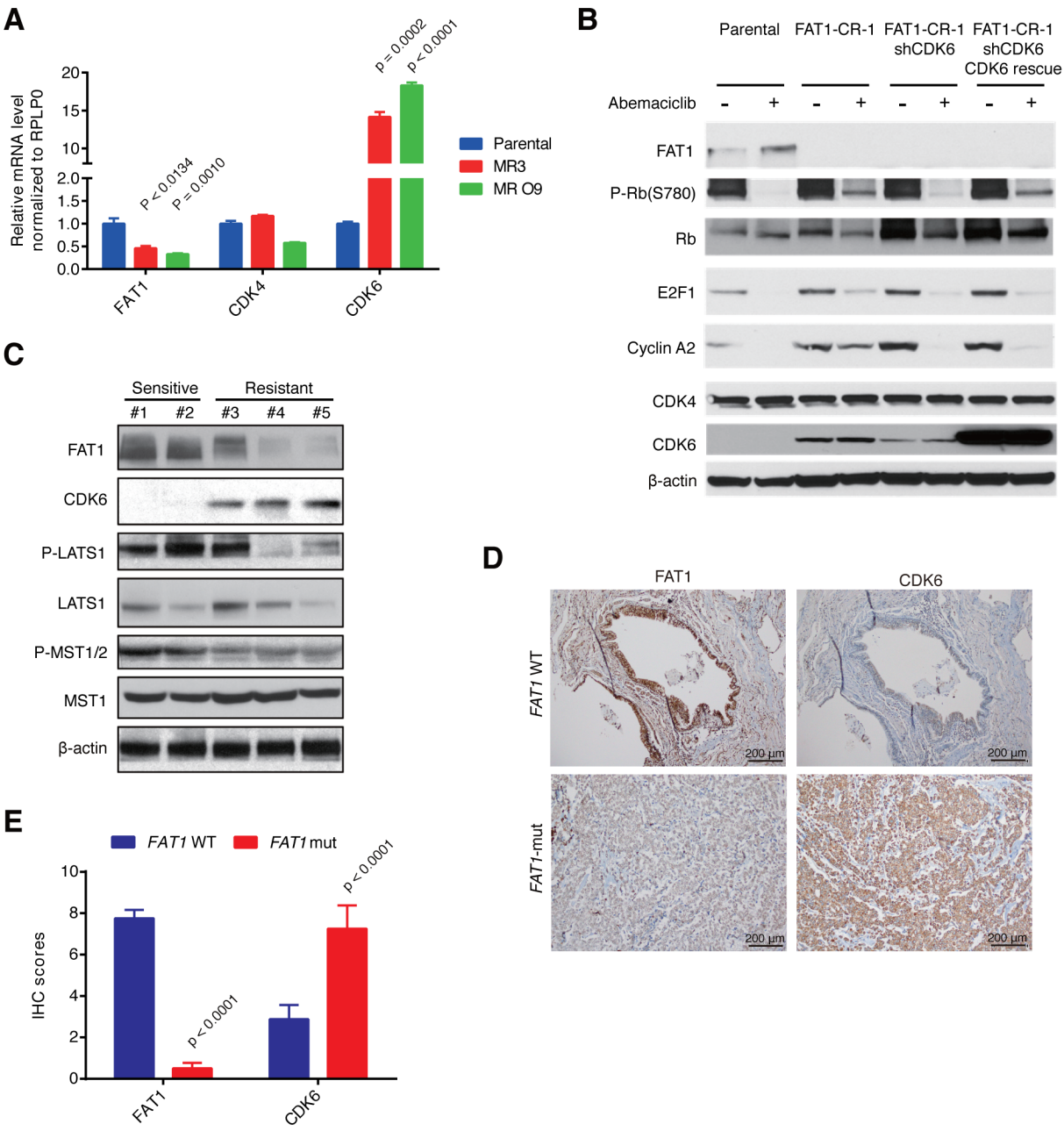

Figure S4, related to Figure 4. The expression of CDK6 is associated with drug sensitivity.

(**A**) Relative mRNA expression of *FAT1*, *CDK4* and *CDK6* were normalized to *RPLP0* in MR3 and MR O9 cells. Data are represented as mean ± SD, n=2. All p values are based on one-way ANOVA test with Dunnett's method correction compared with parental. (**B**) Phospho-Rb levels and protein expression of indicated genes in parental and *FAT1*-loss MCF7 cells constitutively

expressing CDK6-shRNA, or CDK6-shRNA plus CDK6 overexpression. Cells were treated with or without 100 nM of abemaciclib for 24 hours after 48 hours of transfection. (**C**) Immunoblotting of indicated proteins in PDXs treated with ribociclib for 9 weeks reveals significantly lower FAT1 and higher CDK6 expression as well as decreased phosphorylation of Hippo pathway proteins in resistant PDXs compared to sensitive PDXs. (**D**) Immunohistochemical (IHC) images of human breast tumors with different *FAT1* alterations stained with FAT1 or CDK6 antibodies. Scale bars, 200 μm. (**E**) Quantification of FAT1 and CDK6 staining in IHC images of human breast cancers (8 *FAT1* wild-type vs. 8 *FAT1* genomically altered) by a pathologist blinded to the genomic status of the cancers reveals tumors with low FAT1 expression have elevated CDK6 levels. Data are represented as mean + SD. All p values are based on two-tailed unpaired Student's t-tests.

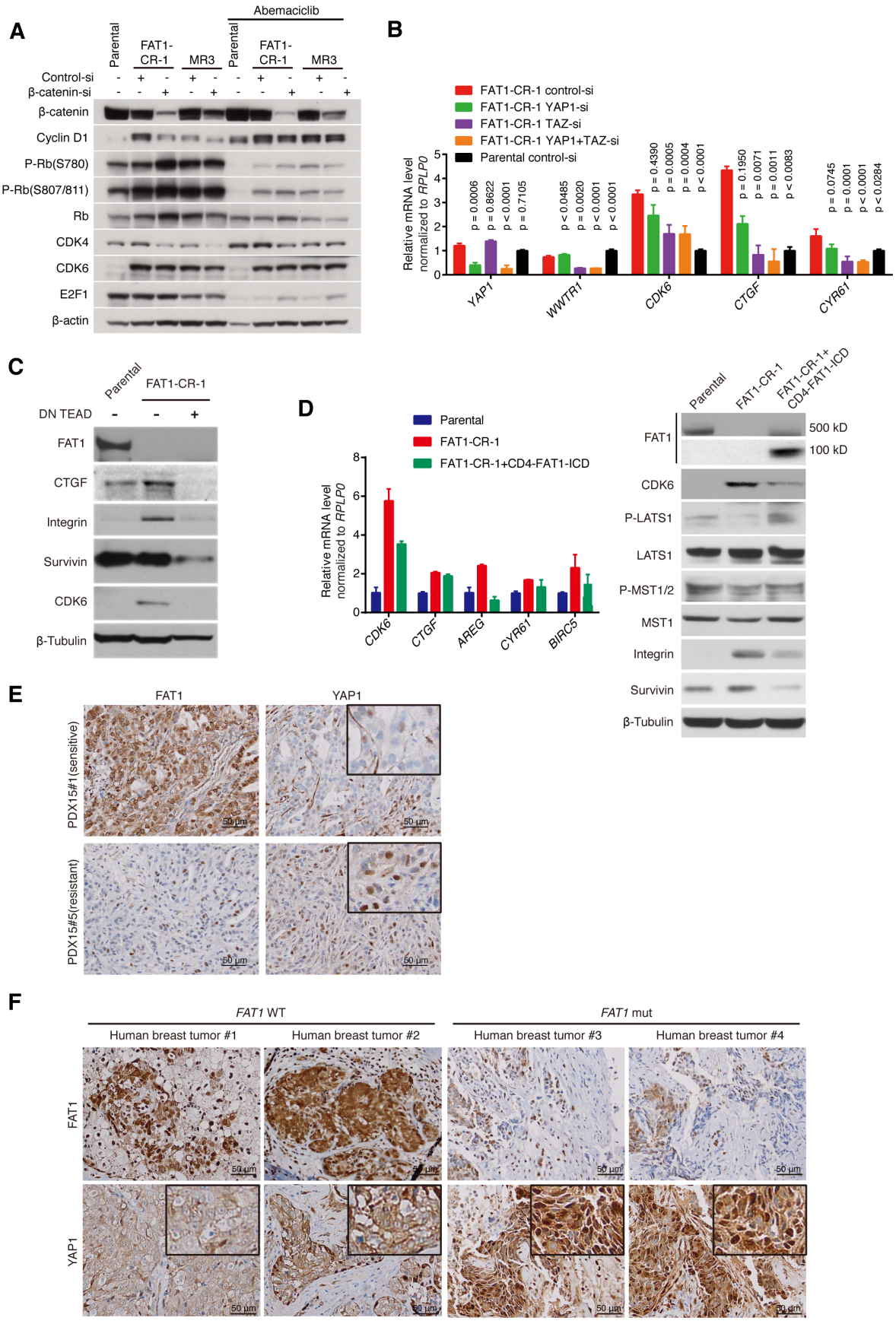
A
Abemaciclib
Parental
FAT1-CR-1
MR3
Parental
FAT1-CR-1
MR3
Control-si
β-catenin-si
β-catenin
Cyclin D1
P-Rb(S780)
P-Rb(S807/811)
Rb
CDK4
CDK6
E2F1
β-actin
B
FAT1-CR-1 control-si
FAT1-CR-1 YAP1-si
FAT1-CR-1 TAZ-si
FAT1-CR-1 YAP1+TAZ-si
Parental control-si
Relative mRNA level normalized to RPLP0
p = 0.0006
p = 0.8622
p < 0.0001
p = 0.7105
p < 0.0485
p = 0.0020
p < 0.0001
p < 0.0001
p = 0.4390
p = 0.0005
p = 0.0004
p < 0.0001
p = 0.1950
p = 0.0071
p = 0.0011
p < 0.0083
p = 0.0745
p = 0.0001
p < 0.0001
p < 0.0284
YAP1
WWTR1
CDK6
CTGF
CYR61
C
Parental
FAT1-CR-1
DN TEAD
FAT1
CTGF
Integrin
Survivin
CDK6
β-Tubulin
D
Parental
FAT1-CR-1
FAT1-CR-1+CD4-FAT1-ICD
Relative mRNA level normalized to RPLP0
CDK6
CTGF
AREG
CYR61
BIRC5
Parental
FAT1-CR-1
FAT1-CR-1+ CD4-FAT1-ICD
FAT1
500 kD
100 kD
CDK6
P-LATS1
LATS1
P-MST1/2
MST1
Integrin
Survivin
β-Tubulin
E
FAT1
YAP1
PDX15#1(sensitive)
PDX15#5(resistant)
50 μm
F
FAT1 WT
FAT1 mut
Human breast tumor #1
Human breast tumor #2
Human breast tumor #3
Human breast tumor #4
FAT1
YAP1
50 μm

Figure S5, related to Figure 5. YAP and TAZ, but not β–catenin, are required for the induction of CDK6

(**A**) Phospho-Rb and expression of indicated proteins in parental and *FAT1* ablation cells with CTNNB1 knockdown. Cells were treated with or without 100 nM of abemaciclib for 24 hours after 48 hours of transfection. (**B**) Relative mRNA expression of indicated genes normalized to *RPLP0* in FAT1-CR and parental MCF7 cells transfected with indicated siRNAs against YAP/TAZ showing *FAT1* loss-mediated induction of CDK6 is YAP/TAZ dependent. Data are represented as mean ± SD, n=3. p values (One-way ANOVA statistical test with Dunnett's method correction, compared with FAT1-CR-1 control-si) were calculated. (**C**) Protein expression of indicated proteins in parental and *FAT1* ablation cells with dominant negative (DN) TEAD overexpression. (**D**) Protein expression and relative mRNA expression of indicated genes in parental MCF7 cells, FAT1-CR cells and FAT1-CR cells overexpressing CD4-FAT1-ICD reveals FAT1 expression suppresses the transcription of CDK6 and Hippo targets. Data are represented as mean ± SD, n=2. (**E**) Immunohistochemical (IHC) images of PDX samples with different sensitivity to CDK4/6 inhibitors stained with FAT1 and YAP1 antibodies reveal increased YAP1 nuclear localization in FAT1-low (resistant) PDX samples. Scale bars 50 μm. A zoom in area of YAP1 staining showed on the up-right corner. (**F**) Immunohistochemical (IHC) images of human breast tumors stained with FAT1 or YAP1 antibodies reveal increased YAP1 nuclear localization in FAT1-low samples. Scale bars 100 μm. A zoom in area of YAP1 staining showed on the up-right corner. (8 *FAT1* wild-type vs. 8 *FAT1* genomically altered)

Table S5, related to Figure 5. RNA sequencing result of parental MCF7 and *FAT1* knockout cells. Some cell cycle related genes are listed below.

ID	Fold change	Adjusted p value	MCF-7_1	MCF-7_2	FAT1 CR_1	FAT1 CR_2
CDK6	2.91	1.02e-56	112.13	99.08	762.79	824.16
FAT1	-4.89	6.31e-29	1189.91	748.99	36.99	28.34
CTGF	2.49	3.21e-02	2.90	3.64	21.99	14.74
CCNA2	1.67	5.56e-12	1547.56	1517.07	2487.32	2640.26
CCND1	1.38	6.77e-08	16492.48	15689.72	22391.92	22116.28
CCND3	0.68	0.0001	1079.72	958.96	715.81	663.18
CCNE1	1.06	0.82	213.62	221.79	224.94	234.66
CCNE2	1.23	0.05	845.79	907.15	1018.72	1137.05